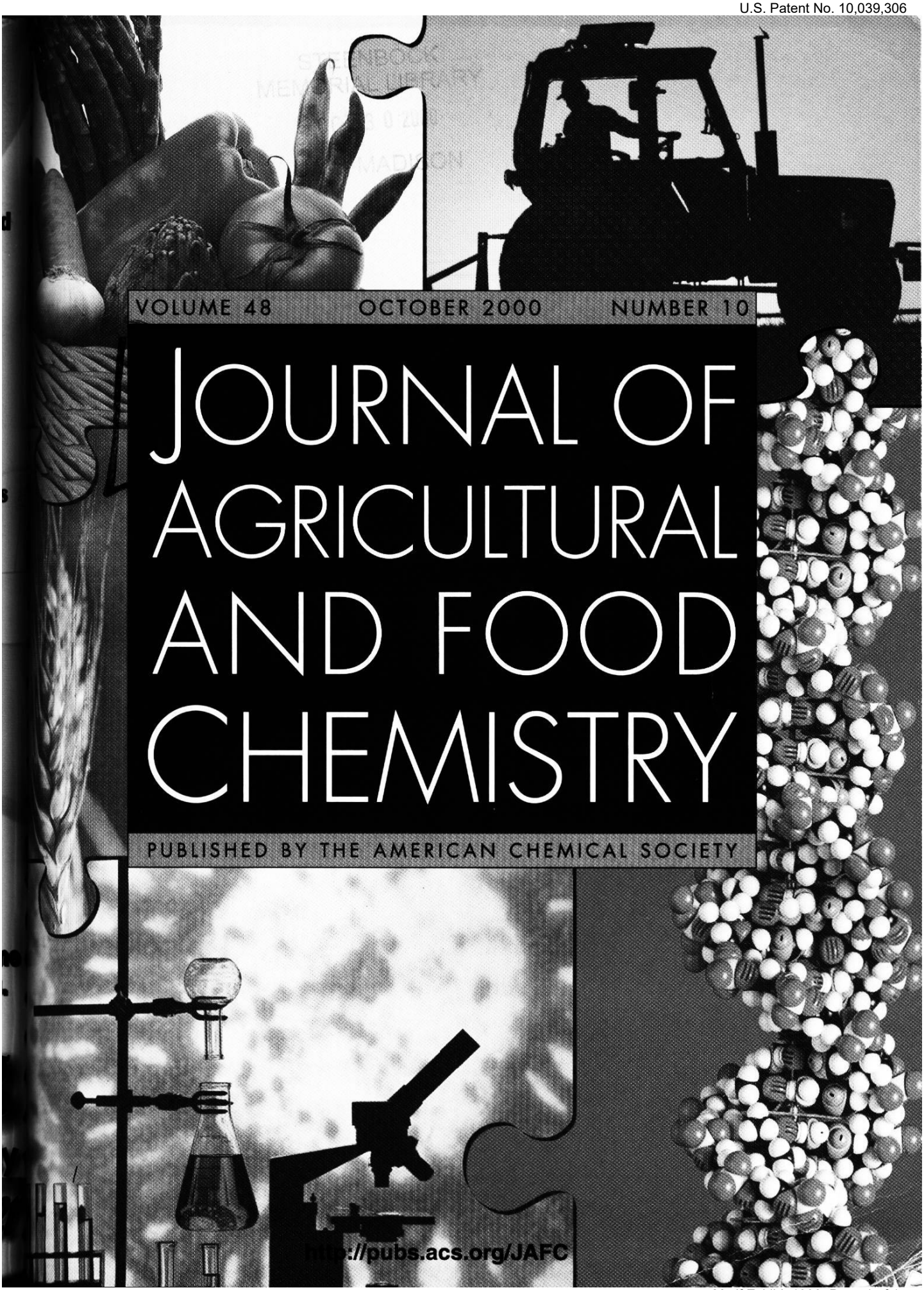
VOLUME 48 OCTOBER 2000 NUMBER 10
JOURNAL OF AGRICULTURAL AND FOOD CHEMISTRY
PUBLISHED BY THE AMERICAN CHEMICAL SOCIETY
http://pubs.acs.org/JAFC

JAFCAU 48(10) 4453–5096 (2000)
ISSN 0021-8561

Registered in U.S. Patent and Trademark Office
Copyright 2000 by the American Chemical Society

OCTOBER 2000

JOURNAL OF AGRICULTURAL AND FOOD CHEMISTRY®

ANALYTICAL METHODS

4453 HAI–RTP Determination of Carbaryl Pesticide in Different Irrigation Water Samples of South Spain
A. Segura-Carretero, C. Cruces-Blanco,* J. F. Fernández-Sánchez, B. Cañabate-Díaz, and A. Fernández-Gutiérrez

4460 Contamination of Italian Citrus Essential Oils: Presence of Chloroparaffin
Giuseppa Di Bella, Marcello Saitta, Simona Lo Curto, Vincenzo Lo Turco, Alessandro Visco, and Giacomo Dugo*

4463 Novel Method for the Discrimination of Tuna (*Thunnus thynnus*) and Bonito (*Sarda sarda*) DNA
Andrew K. Lockley* and Ronald G. Bardsley

4469 Factors Affecting the Collection and Fitting of Nuclear Magnetic Cross-Relaxation Spectroscopy Data with Application to Waxy Corn Starch
Kenneth S. Lewen, Iris H. McCormick, Paul Molitor, Shelly J. Schmidt,* and Thomas M. Eads

4477 Determination of Total Dietary Fiber of Intact Cereal Food Products by Near-Infrared Reflectance
Douglas D. Archibald* and Sandra E. Kays

4487 Determination of Glucosinolates in Canola Seeds Using Anion Exchange Membrane Extraction Combined with the High-Pressure Liquid Chromatography Detection
Anna M. Szmigielska,* Jeff J. Schoenau, and Vanessa Levers

4492 Hapten Synthesis for the Development of a Competitive Inhibition Enzyme-Immunoassay for Thiram
Françoise Gueguen, Frédéric Boisdé, Anne-Laurence Queffelec, Jean-Pierre Haelters, Daniel Thouvenot, Bernard Corbel, and Patrice Nodet*

4500 Analytical Method for the Determination of Atrazine and Its Dealkylated Chlorotriazine Metabolites in Water Using Gas Chromatography/Mass Selective Detection
Robert A. Yokley* and Max W. Cheung

4508 Rapid and Sensitive Determination of 4-Nitrophenol, 3-Methyl-4-nitrophenol, 4,6-Dinitro-*o*-cresol, Parathion-methyl, Fenitrothion, and Parathion-ethyl by Liquid Chromatography with Electrochemical Detection
Teresa Galeano-Díaz,* Agustina Guiberteau-Cabanillas, Nielene Mora-Díez, Piedad Parrilla-Vázquez, and Francisco Salinas-López

4514 Continuous Sorbent Preconcentration for the Electrothermal Atomic Absorption Spectrometric Determination of Ultratrace Amounts of Cobalt in Milled Wheat Fractions
M. Mar González, Mercedes Gallego, and Miguel Valcárcel*

4520 Development of Enzyme-Linked Immunosorbent Assays for Toxic Larkspur (*Delphinium* spp.) Alkaloids
Stephen T. Lee,* Thomas K. Schoch, Dale R. Gardner, and Bryan L. Stegelmeier

Case No.: IPR2023-00209
U.S. Patent No. 10,039,306

BIOTECHNOLOGY

4529 Cleavage of the Diketonitrile Derivative of the Herbicide Isoxaflutole by Extracellular Fungal Oxidases
Christian Mougin,* François-Didier Boyer, Eliane Caminade, and Rachel Rama

4535 Irreversible Unfolding of Myoglobin in an Aqueous Solution by Supercritical Carbon Dioxide
Hiroya Ishikawa,* Mitsuya Shimoda, Akiyoshi Yonekura, Keiko Mishima, Kiyoshi Matsumoto, and Yutaka Osajima

4540 Microassay for Rapid Screening of α-Amylase Activity
Dominic W. S. Wong,* Sarah B. Batt, and George H. Robertson

4544 Thermal Dependence of Malate Synthase Activity and Its Relationship to the Thermal Dependence of Seedling Emergence
James R. Mahan

4550 Conversion to Docosahexaenoic Acid-Containing Phosphatidylserine from Squid Skin Lecithin by Phospholipase D-Mediated Transphosphatidylation
Masashi Hosokawa,* Tatuya Shimatani, Teruyuki Kanada, Yoshikazu Inoue, and Koretaro Takahashi

4555 Immunochemical Evaluation of Bovine β-Casein and Its 1−28 Phosphopeptide in Cheese during Ripening
Rosa Pizzano,* Maria Adalgisa Nicolai, Pierfrancesco Padovano, Pasquale Ferranti, Francesca Barone, and Francesco Addeo

4561 Antifungal and Peroxidative Activities of Nonheme Chloroperoxidase in Relation to Transgenic Plant Protection
T. J. Jacks,* A. J. De Lucca, K. Rajasekaran, K. Stromberg, and K.-H. van Pée

CHEMICAL CHANGES DURING PROCESSING/STORAGE

4565 Ellagic Acid, Vitamin C, and Total Phenolic Contents and Radical Scavenging Capacity Affected by Freezing and Frozen Storage in Raspberry Fruit
Begoña de Ancos, Eva M. González, and M. Pilar Cano*

4571 Ultraviolet C Irradiation at 0.5 $kJ \cdot m^{-2}$ Reduces Decay without Causing Damage or Affecting Postharvest Quality of Star Ruby Grapefruit (*C. paradisi* Macf.)
Guy D'hallewin, Mario Schirra,* Mario Pala, and Shimshon Ben-Yehoshua

4576 Effect of Enzymatic and Chemical Oxidation on the Antioxidant Capacity of Catechin Model Systems and Apple Derivatives
Maria Cristina Nicoli, Sonia Calligaris,* and Lara Manzocco

4581 Antioxidant Activity of Pomegranate Juice and Its Relationship with Phenolic Composition and Processing
María I. Gil, Francisco A. Tomás-Barberán, Betty Hess-Pierce, Deirdre M. Holcroft, and Adel A. Kader*

4590 Contribution of Periderm Material and Blanching Time to the Quality of Pasteurized Peach Puree
S. T. Talcott, L. R. Howard,* and C. H. Brenes

4597 Effects of Pulsed Electric Fields on the Quality of Orange Juice and Comparison with Heat Pasteurization
Hye Won Yeom, Charles B. Streaker, Q. Howard Zhang,* and David B. Min

4606 Effect of Postharvest Ultraviolet Irradiation on Resveratrol and Other Phenolics of Cv. Napoleon Table Grapes
Emma Cantos, Cristina García-Viguera, Sonia de Pascual-Teresa, and Francisco A. Tomás-Barberán*

4613 Behavior of Monosaccharides, Phenolic Compounds, and Color of Red Wines Aged in Used Oak Barrels and in the Bottle
María del Alamo, José Luis Bernal, and Carmen Gómez-Cordovés*

4619 Fining Treatments of White Wines by Means of Polymeric Adjuvants for Their Stabilization against Browning
Giovanni Spagna,* Riccardo N. Barbagallo, and Pier Giorgio Pifferi

4628 Estrogenic Effects of Extracts from Cabbage, Fermented Cabbage, and Acidified Brussels Sprouts on Growth and Gene Expression of Estrogen-Dependent Human Breast Cancer (MCF-7) Cells
Young H. Ju, Kathy E. Carlson, Jun Sun, Dorothy Pathak, Benita S. Katzenellenbogen, John A. Katzenellenbogen, and William G. Helferich*

Case No.: IPR2023-00209
U.S. Patent No. 10,039,306

4635 Autoxidation of Packed Almonds as Affected by Maillard Reaction Volatile Compounds Derived from Roasting
Carla Severini,* Tommaso Gomes, Teresa De Pilli, Santina Romani, and Roberto Massini

4641 Biological Response of Rats Fed with Tofu Treated with High Hydrostatic Pressure
Préstamo, G.* and Arroyo, G.

4647 Optimal Conditions for Phytate Degradation, Estimation of Phytase Activity, and Localization of Phytate in Barley (Cv. Blenheim)
Eva-Lotta Bergman,* Karin Autio, and Ann-Sofie Sandberg

CHEMISTRY OF CROP AND ANIMAL PROTECTION

4656 Novel Procedure for Identification of Compounds Inhibitory to Transcription of Genes Involved in Mycotoxin Biosynthesis
Seanna L. Annis, Luis Velasquez, Haixin Xu, Ray Hammerschmidt, John Linz, and Frances Trail*

4661 Elucidation of Fipronil Photodegradation Pathways
Kenley K. Ngim, Scott A. Mabury, and Donald G. Crosby*

4666 Reduction of Pesticide Residues on Produce by Rinsing
■ **Walter J. Krol,* Terri L. Arsenault, Harry M. Pylypiw, Jr., and Mary Jane Incorvia Mattina**

4671 Simultaneous Derivatization and Trapping of Volatile Products from Aqueous Photolysis of Thiamethoxam Insecticide
Barb J. Schwartz,* F. Kay Sparrow, Nina E. Heard, and Bruce M. Thede

4676 In Vitro and in Situ Inhibition of Carotenoid Biosynthesis in *Capsicum annuum* by Bleaching Herbicides
Andrew J. Simkin, Jürgen Breitenbach, Marcel Kuntz,* and Gerhard Sandmann

4681 Influence of Metam Sodium on the Dissipation and Residual Biological Activity of the Herbicides EPTC and Pebulate in Surface Soil under Black Plastic Mulch
Carrie L. Stiles, Carl E. Sams, Darren K. Robinson, David L. Coffey, and Thomas C. Mueller*

4687 Isolation and Characterization of Fungal Inhibitors from *Epichloë festucae*
Qin Yue, Christina J. Miller, James F. White, Jr., and Michael D. Richardson*

4693 Identification of Metabolites of [1,2,3-^{13}C]Propargyl Alcohol in Mouse Urine by ^{13}C NMR and Mass Spectrometry and Comparison to Rat
Ali R. Banijamali,* Yaodong Xu, Vincent DeMatteo, and Richard J. Strunk, and Susan J. Sumner

4711 Effects of pH on Chemical Stability and De-esterification of Fenoxaprop-ethyl by Purified Enzymes, Bacterial Extracts, and Soils
Robert M. Zablotowicz,* Robert E. Hoagland, William J. Staddon, and Martin A. Locke

4717 Comparative Toxicity of Selected Organophosphate Insecticides against Resistant and Susceptible Clones of the Greenbug, *Schizaphis graminum* (Homoptera: Aphididae)
Jian-Rong Gao and Kun Yan Zhu*

COMPOSITION OF FOODS/FEEDS/BIOBASED PRODUCTS

4723 Antioxidative Activity and Carotenoid and Tomatine Contents in Different Typologies of Fresh Consumption Tomatoes
C. Leonardi,* P. Ambrosino, F. Esposito, and V. Fogliano

4728 Phlorin Screening in Various Citrus Species and Varieties
Laurence M.-M. Louche, François Luro, Emile M. Gaydou,* and Jean-Claude Lesage

4734 Identification by HPLC−DAD and HPLC−MS Analyses and Quantification of Constituents of Fennel Teas and Decoctions
Anna Rita Bilia,* Margherita Fumarola, Sandra Gallori, Giovanni Mazzi, and F. F. Vincieri

Motif Exhibit 1093, Page 4 of 17

Case No.: IPR2023-00209
U.S. Patent No. 10,039,306

4739 Long-Chain Aliphatic β-Diketones from Epicuticular Wax of *Vanilla* Bean Species. Synthesis of Nervonoylacetone
Béatrice Ramaroson-Raonizafinimanana, Emile M. Gaydou,* and Isabelle Bombarda

4744 Flavonoids in Monospecific *Eucalyptus* Honeys from Australia
Isabel Martos, Federico Ferreres, Lihu Yao, Bruce D'Arcy, Nola Caffin, and Francisco A. Tomás-Barberán*

4749 Foliar Application of Selenite and Selenate to Potato (*Solanum tuberosum*): Effect of a Ligand Agent on Selenium Content of Tubers
Valeria Poggi,* Alberto Arcioni, Paola Filippini, and Pier Giorgio Pifferi

ENVIRONMENTAL CHEMISTRY

4752 Behavior of Four Sulfonylurea Herbicides in the Presence of Hydroxy Compounds
Jean Sabadie

4757 Effect of Temperature and Moisture on the Degradation and Sorption of Florasulam and 5-Hydroxyflorasulam in Soil
Mark S. Krieger,* Fiona Pillar, and Julie A. Ostrander

4767 Organo-Clay Formulations of the Hydrophobic Herbicide Norflurazon Yield Reduced Leaching
Tomás Undabeytia,* Shlomo Nir, and Baruch Rubin

4774 Photostabilization of the Herbicide Norflurazon by Using Organoclays
Tomás Undabeytia,* Shlomo Nir, Elisha Tel-Or, and Baruch Rubin

4780 Adsorption–Desorption Studies of Selected Herbicides in Soil–Fly Ash Mixtures
I. K. Konstantinou and T. A. Albanis*

4791 Montmorillonite–Phenyltrimethylammonium Yields Environmentally Improved Formulations of Hydrophobic Herbicides
Yasser El-Nahhal,* Shlomo Nir, Carina Serban, Onn Rabinovitch, and Baruch Rubin

FLAVORS AND AROMAS

4802 Aroma Potential of Two Bairrada White Grape Varieties: Maria Gomes and Bical
S. Rocha,* P. Coutinho, A. Barros, M. A. Coimbra, I. Delgadillo, and A. Dias Cardoso

4808 Structured Fluids as Microreactors for Flavor Formation by the Maillard Reaction
S. Vauthey, Ch. Milo, Ph. Frossard, N. Garti, M. E. Leser, and H. J. Watzke*

4817 Determination of Antioxidant Properties of Aroma Extracts from Various Beans
Kwang-Geun Lee, Alyson E. Mitchell, and Takayuki Shibamoto*

4821 9-Hydroxypiperitone β-D-Glucopyranoside and Other Polar Constituents from Dill (*Anethum graveolens* L.) Herb
Bernd Bonnländer and Peter Winterhalter*

4826 Biotransformation of (−)-Dihydromyrcenyl Acetate Using the Plant Parasitic Fungus *Glomerella cingulata* as a Biocatalyst
Mitsuo Miyazawa,* Shin-ichi Akazawa, Hiromu Sakai, and Hirokazu Nankai

4830 Organoleptic Impact of 2-Methoxy-3-isobutylpyrazine on Red Bordeaux and Loire Wines. Effect of Environmental Conditions on Concentrations in Grapes during Ripening
Dominique Roujou de Boubée, Cornelis Van Leeuwen, and Denis Dubourdieu*

4835 Identification and Quantification of Geosmin, an Earthy Odorant Contaminating Wines
Philippe Darriet,* Monique Pons, Sophie Lamy, and Denis Dubourdieu

4839 Development and Characterization of a Flavoring Agent from Oyster Cooker Effluent
D. S. Kim, H. H. Baek, C. B. Ahn, D. S. Byun, K. J. Jung, H. G. Lee, K. R. Cadwallader, and H. R. Kim*

4844 Volatile Compounds in the Production of Liquid Beet Sugar
Per Pihlsgård,* Mats Larsson, Anders Leufvén, and Hans Lingnert

4851 Aroma of Fresh Oysters *Crassostrea gigas*: Composition and Aroma Notes
F. Piveteau, S. Le Guen, G. Gandemer, J.-P. Baud, C. Prost, and M. Demaimay*

Case No.: IPR2023-00209
U.S. Patent No. 10,039,306

4858 Dynamic Headspace Gas Chromatography/Mass Spectrometry Characterization of Volatiles Produced in Fish Oil Enriched Mayonnaise during Storage
Karsten Hartvigsen,* Pia Lund, Lotte F. Hansen, and Gunhild Hølmer

4868 Composition of the Essential Oil of *Citrus tamurana* Hort. ex Tanaka (Hyuganatsu)
Hyang-Sook Choi and Masayoshi Sawamura*

FOOD CHEMISTRY/BIOCHEMISTRY

4874 Activities of Antioxidants Are Affected by Colloidal Properties of Oil-in-Water and Water-in-Oil Emulsions and Bulk Oils
Karin Schwarz,* Shu-Wen Huang, J. Bruce German, Brigitte Tiersch, Jürgen Hartmann, and Edwin N. Frankel

4883 Simple Rapid Procedure for Preparation of Large Quantities of Ovalbumin
Thomas Croguennec, Françoise Nau,* Stéphane Pezennec, and Gérard Brule

4890 Approaches to Wine Aroma: Release of Aroma Compounds from Reactions between Cysteine and Carbonyl Compounds in Wine
Stéphanie Marchand, Gilles de Revel,* and Alain Bertrand

4896 Effect of Storage Temperature on the Degradation of Dimethoate in Fortified Orange and Peach Juices
Panagiotis Athanasopoulos,* Nikolaos B. Kyriakidis, and Ioulia Georgitsanakou

4900 Tetrahydro-β-carbolines, Potential Neuroactive Alkaloids, in Chocolate and Cocoa
Tomas Herraiz*

4905 Early Structural Changes in Myosin Rod upon Heating of Carp Myofibrils
Kunihiko Konno,* Takeshi Yamamoto, Masayuki Takahashi, and Sanae Kato

4910 Inhibition of Formation of Oxidative Volatile Components in Fermented Cucumbers by Ascorbic Acid and Turmeric
A. Zhou, R. F. McFeeters,* and H. P. Fleming

4913 Tryptophan-*N*-glucoside in Fruits and Fruit Juices
Stefanie Diem, Jochen Bergmann, and Markus Herderich*

4918 Separation of Thermostable Pectinmethylesterase from Marsh Grapefruit Pulp
Milena Corredig, William Kerr, and Louise Wicker*

4924 Antioxidative Activity in the Pericarp and Seed of Japanese Pepper (*Xanthoxylum piperitum* DC)
Eika Hisatomi, Mikiko Matsui, Akio Kobayashi, and Kikue Kubota*

4929 β-Glucosidases from Five Black *Aspergillus* Species: Study of Their Physico-Chemical and Biocatalytic Properties
Claudia H. Decker, Jaap Visser, and Peter Schreier*

4937 Solubility, Tensile, and Color Properties of Modified Soy Protein Isolate Films
Jong W. Rhim, Aristippos Gennadios,* Akihiro Handa, Curtis L. Weller, and Milford A. Hanna

4942 Reaction Rate Modeling in Cryoconcentrated Solutions: Alkaline Phosphatase Catalyzed DNPP Hydrolysis
Dominique Champion,* Genevieve Blond, Martine Le Meste, and Denise Simatos

4948 Molecular Characterization around a Glassy Transition of Starch Using ^{1}H Cross-Relaxation Nuclear Magnetic Resonance
Yael Vodovotz,* L. Charles Dickinson, and Pavinee Chinachoti

4955 Fluorescence of Raw Cane Sugars Evaluated by Chemometrics
Dorrit Baunsgaard, Lars Nørgaard,* and Mary An Godshall

4963 Oxidative in Vitro Metabolism of the Soy Phytoestrogens Daidzein and Genistein
Sabine E. Kulling,* Doris M. Honig, Thomas J. Simat, and Manfred Metzler

4973 Lactones. 9. Synthesis of Terpenoid Lactones—Active Insect Antifeedants
Edyta Paruch, Zbigniew Ciunik, Jan Nawrot, and Czesław Wawrzeńczyk*

4978 Glutathione Reductase in Wheat Grain. 1. Isolation and Characterization
Frédéric de Lamotte, Nicolas Vianey-Liaud, Marie-Pierre Duviau, and Károly Kobrehel*

Motif Exhibit 1093, Page 6 of 17

Case No.: IPR2023-00209
U.S. Patent No. 10,039,306

4984 Lactoferrin in Infant Formulas: Effect on Oxidation
M. Teresa Satué-Gracia, Edwin N. Frankel,* Nagendra Rangavajhyala, and J. Bruce German

4991 Purification and Characterization of an Esterase Conferring Resistance to Fenitrothion in *Oryzaephilus surinamensis* (L.) (Insecta, Coleoptera, Silvanidae)
Sung-Eun Lee,* Edith M. Lees, and Bruce C. Campbell

4997 Honeys from Different Floral Sources as Inhibitors of Enzymatic Browning in Fruit and Vegetable Homogenates
Lei Chen, Amar Mehta, May Berenbaum, Arthur R. Zangerl, and Nicki J. Engeseth*

5001 Formation of Disulfide Bonds in Acid-Induced Gels of Preheated Whey Protein Isolate
Arno C. Alting,* Rob J. Hamer, Cees G. de Kruif, and Ronald W. Visschers

5008 Effects of Ozone and Oxygen on the Degradation of Carotenoids in an Aqueous Model System
Leola K. Henry, Ni Luh Puspitasari-Nienaber, Manuel Jarén-Galán, Richard B. van Breemen, George L. Catignani, and Steven J. Schwartz*

5014 Purification and Biochemical Properties of Dipeptidyl Peptidase I from Porcine Skeletal Muscle
Miguel Angel Sentandreu and Fidel Toldrá*

5023 Purification and Structural Characterization of LTP1 Polypeptides from Beer
Sandrine Jégou, Jean-Paul Douliez,* Daniel Mollé, Patrick Boivin, and Didier Marion

5030 Comparison of Antioxidant and Antimicrobial Activities of Tilia (*Tilia Argentea Desf Ex DC*), Sage (*Salvia Triloba L.*), and Black Tea (*Camellia Sinensis*) Extracts
Ali Yıldırım,* Ahmet Mavi, Münir Oktay, Ayşe Aydan Kara, Ömer Faruk Algur, and Vahit Bilaloğlu

5035 Toward the Authentication of Varietal Wines by the Analysis of Grape (*Vitis vinifera* L.) Residual DNA in Must and Wine Using Microsatellite Markers
R. Siret,* J. M. Boursiquot, M. H. Merle, J. C. Cabanis, and P. This

5041 Latent Polyphenol Oxidases from Sago Log (*Metroxylon sagu*): Partial Purification, Activation, and Some Properties
Galila Hassan Onsa, Nazamid bin Saari,* Jinap Selamat, and Jamilah Bakar

5046 Effects of Sugars on Whey Protein Isolate Gelation
Lezli M. Rich and E. Allen Foegeding*

5053 Addition of Sugars Influences Color of Oil-in-Water Emulsions
Jochen Weiss* and Wayne Liao

NUTRITIONAL ACTIVITY

5061 Decreased Superoxide Anion Production in Cultured Human Promonocyte Cells (THP-1) Due to Polyphenol Mixtures from Olive Oil Processing Wastewaters
Claude L. Léger,* Najib Kadiri-Hassani, and Bernard Descomps

5068 Antioxidative Activity of Green Tea Treated with Radical Initiator 2,2′-Azobis(2-amidinopropane) Dihydrochloride
Takako Yokozawa,* Eun Ju Cho, Yukihiko Hara, and Kenichi Kitani

SAFETY/TOXICOLOGY

5074 Antimutagenic Activity of Cacao: Inhibitory Effect of Cacao Liquor Polyphenols on the Mutagenic Action of Heterocyclic Amines
Megumi Yamagishi,* Midori Natsume, Atsushi Nagaki, Toko Adachi, Naomi Osakabe, Toshio Takizawa, Harue Kumon, and Toshihiko Osawa

5079 Production of Polyclonal Antibodies against Ochratoxin A and Its Detection in Chilies by ELISA
K. Thirumala-Devi, M. A. Mayo, Gopal Reddy, S. V. Reddy, P. Delfosse, and D. V. R. Reddy*

5083 Polycyclic Aromatic Hydrocarbons in Liquid Smoke Flavorings Obtained from Different Types of Wood. Effect of Storage in Polyethylene Flasks on Their Concentrations
María Dolores Guillén,* Patricia Sopelana, and María Aránzazu Partearroyo

Motif Exhibit 1093, Page 7 of 17

Case No.: IPR2023-00209
U.S. Patent No. 10,039,306

5088 Investigation on the Possible Formation of *N*-Nitroso-*N*-methylurea by Nitrosation of Creatinine in Model Systems and in Cured Meats at Gastric pH

Nrisinha P. Sen,* Stephen W. Seaman, Christine Burgess, Philander A. Baddoo, and Dorcas Weber

■ Supporting Information is available free of charge via the Internet at http://pubs.acs.org.

* In papers with more than one author, the asterisk indicates the name of the author to whom inquiries about the paper should be addressed.

Motif Exhibit 1093, Page 8 of 17

Case No.: IPR2023-00209
U.S. Patent No. 10,039,306

Structured Fluids as Microreactors for Flavor Formation by the Maillard Reaction

This material may be protected by Copyright law (Title 17 U.S. Code)

S. Vauthey, Ch. Milo, Ph. Frossard, N. Garti, M. E. Leser, and H. J. Watzke*

Nestlé Research Centre, Nestec Ltd., Vers-chez-les-Blanc, P.O. Box 44, 1000 Lausanne 26, Switzerland

Thermal reactions of cysteine/furfural and cysteine/ribose mixtures were studied in model systems to gain more insight into the influence of structured fluids such as L_2 microemulsions and cubic phases on the generation of aroma compounds. Formation of 2-furfurylthiol from cysteine/furfural was particularly efficient in L_2 microemulsions and cubic phases compared to aqueous systems. The reaction led to the formation of two new sulfur compounds, which were identified as 2-(2-furyl)-thiazolidine and, tentatively, *N*-(2-mercaptovinyl)-2-(2-furyl)thiazolidine. Similarly, generation of 2-furfurylthiol and 2-methyl-3-furanthiol from cysteine/ribose mixtures was strongly enhanced in structured fluids. The cubic phase was shown to be even more efficient in flavor generation than the L_2 microemulsion. It was denoted "cubic catalyst" or "cubic selective microreactor". The obtained results are interpreted in terms of a surface and curvature control of the reactions defined by the structural properties of the formed surfactant associates.

Keywords: *Microemulsion; cubic phase; structured fluids; Maillard reaction; formation of thiols; flavor precursors; 2-furfurylthiol*

INTRODUCTION

Maillard reactions, for example, thermally induced reactions of amino acids and reducing sugars, have been studied for a long time, also with respect to their potential to generate flavors. It should be emphasized that the thermal reaction between cysteine and carbohydrates leads to the formation of >200 volatile compounds (Mulders, 1973; Farmer et al., 1989; Mottram and Whitfield, 1995). Of particular interest is the generation of sulfur-containing aroma compounds such as 2-furfurylthiol (FFT) and 2-methyl-3-furanthiol (MFT). Both compounds are potent odorants with unique sensory properties and were determined by aroma extract dilution analysis (AEDA) as major contributors to the aroma of a wide variety of food products including coffee (Holscher et al., 1990), cooked beef (Gasser and Grosch, 1988), and roasted sesame seeds (Schieberle, 1993). It was also shown that FFT and MFT belong to the key impact compounds of heated cysteine/ribose mixtures (Hofmann and Schieberle, 1995). Quantitation of these compounds by stable isotope dilution assays in dry-heated and aqueous reaction systems revealed a strong influence of the reaction conditions on the concentrations of these potent odorants (Schieberle and Hofmann, 1998). Particularly, the formation of FFT was strongly enhanced under the conditions of dry heating, which reflected roasting conditions. Other parameters affecting their generation, such as pH dependence, have also been studied (Schieberle and Hofmann, 1996), as well as the effectiveness of different sugar-derived degradation products as precursors (Hofmann and Schieberle, 1996). Furfural, a thermal pentose sugar degradation product, was shown to be an intermediate in the formation of FFT (Münch et al., 1997) and was chosen in our study to gain more insight into the influence of structured media on the generation of aroma compounds. The use of model systems is the primary tool to investigate the effect of structured fluids on the Maillard reaction.

Structured fluids are generally composed of microstructures dispersed in a homogeneous phase. Much attention was given in the past to association colloids, that is, aggregates formed by amphiphilic molecules (Hiemenz, 1986; Larsson, 1994; Laughlin, 1994) such as micelles, vesicles, microemulsions, mesophases, and macromolecule self-assemblies.

Monoglycerides were used in this work as surfactant for the generation of association colloids used as microreactors for the Maillard reactions. Monoglycerides consist of a single acyl chain (hydrophobic tail), which is attached to a glycerol moiety (hydrophilic headgroup). The headgroup is only weakly hydrated. The acyl chain of the monoglycerides may differ in the degree of unsaturation: It can be totally saturated or have either one (e.g., oleic acid) or two (e.g., linoleic acid) double bonds. When dispersed in water, monoglycerides are known to exhibit a rich polymorphism; that is, they form up to six distinct phases depending on the water content and the temperature (Krog, 1997; Briggs et al., 1996; Boyle and German, 1996). The degree of unsaturation mainly determines at which temperature the different phases are formed. For instance, with the saturated monoglycerides the cubic phase is formed only at high temperatures (>70−80 °C), whereas in the presence of unsaturated monoglycerides, it is formed at room temperature (see Figure 1). Moreover, the formation of a microemulsion phase (isotropic fluid) at high temperatures is best achieved with unsaturated monoglycerides. The structures of the different phases have been investigated by a variety of techniques, such as small-angle X-ray scattering (SAXS), small-angle neutron scattering (SANS), and microscopy. Because they have both a

* Author to whom correspondence should be addressed (telephone +21/785-8026; fax +21/785-8554; e-mail heribert.watzke@rdls.nestle.ch).

10.1021/jf991254a CCC: $19.00 © 2000 American Chemical Society
Published on Web 09/07/2000

Case No.: IPR2023-00209
U.S. Patent No. 10,039,306

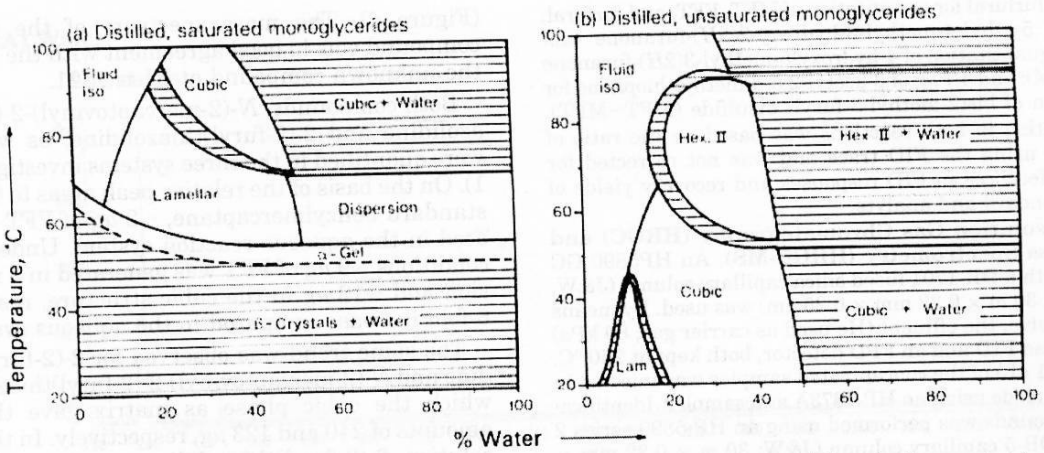

Figure 1. Phase diagrams of distilled monoglyceride products from Danisco Ingredients: (a) from hydrogenated lard (Dimodan P); (b) from sunflower oil (Dimodan LS); adapted from Danisco Ingredients, technical paper TP3-1e.

hydrophobic site (tail region) and a hydrophilic site (headgroup region including the solubilized water region), they are capable of dissolving both water-soluble and oil-soluble compounds (Engstrom, 1990; Ericsson et al., 1991).

Of particular interest is the cubic phase, which has a bicontinuous structure. It is generally described as two interpenetrating networks of water channels separated by a curved bilayer, extending in three dimensions [forming the so-called infinite periodic minimal surface (Larsson, 1989)]. The water pore diameter has been shown to be ~5 nm for the fully swelled phase. The curved bilayer structure gives rise to a very large interfacial area (~400 m^2/g), which is an excellent entrapment medium (Ericsson et al., 1991). The solubilization capacity for organic compounds was found to be governed by various factors but mostly by the curvature of the interface and the degree of water swelling (Ericsson et al., 1983, 1991; Razumas et al., 1996; Caboi et al., 1997).

Bicontinuous cubic phases are optically isotropic and completely transparent and have a consistency like gels, exhibiting the highest viscosity of all of the mesophases formed (Larsson, 1989; Fontell, 1990). Cubic phases can be also in equilibrium with an excess of water (they do not transform into other phases upon contact with water, see Figure 1), which is particularly interesting as a matrix system for a controlled release of drugs and eventually for flavor compounds. In certain cases, even stereoselectivity of organic reactions was achieved at such interfaces (Holmberg, 1994).

Much has been written on the solubilization capacity of cubic phases and on their potential as delivery systems (Burrows et al., 1994; Osborne and Ward, 1995; Chang and Bodmeier, 1997). However, their potential as microreactors for the thermal generation of aromas has not yet been studied. The aim of this work was to compare, on a quantitative basis, the reaction products of cysteine/furfural and cysteine/ribose model systems performed in two different structured fluids, that is, a cubic phase and a microemulsion phase, and in an aqueous medium under the same conditions. The influence of the structured phases on the thermal reactions is discussed.

EXPERIMENTAL PROCEDURES

Chemicals. L-Cysteine, D-ribose, furan-2-aldehyde (furfural), 5-methylfurfural, 5-ethyl-4-methyl-3-hydroxy-2(5*H*)-furanone (abhexon), and 3-acetyl-2,5-dimethylthiophene were obtained from Fluka (Buchs, Switzerland). Dimodan LS (sunflower oil monoglyceride, >98%) and Dimodan PV (saturated vegetable oil monoglyceride, >98%) were kindly provided by Danisco Ingredients (Braband, Denmark). Water used in these experiments was twice distilled.

Model Reactions. L-Cysteine (2 mmol) and furfural (2 mmol) were dissolved in a phosphate buffer (10 mL; 0.5 M; pH 5.0). The cubic phase was prepared by introducing 1 g of this solution and 4 g of melted (60 °C) Dimodan PV (saturated monoglyceride) into a Pyrex tube (i.d. = 1.5 cm). After vigorous stirring (Vortex), the tube was placed in an oil bath at 140 °C for 1 min and stirred again to form a homogeneous cubic phase. Finally, this system was thermally treated for 4 h at 100 °C. To obtain a microemulsion (isotropic fluid) at this temperature, Dimodan PV was replaced by the unsaturated monoglyceride product Dimodan LS ($C_{18:2}$ = 67% and $C_{18:1}$ = 21%; Krog, 1998). As reference, an identical thermal treatment was applied to 1 g of the buffer solution containing the reactants. After heating, the mixture was cooled and 4 g of melted Dimodan PV was added in order to have similar workup conditions for the isolation of volatiles.

In a second series of experiments, L-cysteine (6.67 mmol) and D-ribose (20 mmol) were dissolved in a phosphate buffer (10 mL; 0.5 M; pH 5.0). Cubic phase samples were prepared by introducing 2 g of this solution and 8 g of melted (60 °C) Dimodan PV into a Pyrex tube (i.d. = 2 cm). Finally, this system or 2 g of buffer solution alone (reference) was thermally treated following the same procedure as mentioned above.

Isolation of Volatiles from the Reaction Mixtures. The aqueous reference samples were first transformed into a cubic phase by adding melted Dimodan PV (4 g) to the reaction system to ensure maximal similarity in the reaction mixtures before sample cleanup. After cooling, the mix was extracted with diethyl ether (three times, total of 50 mL). The slurries were combined and submitted to the vacuum transfer system described by Sen et al. (1991) using only two cold traps immersed in liquid nitrogen. Once the sample was entirely frozen in liquid nitrogen, the vacuum was opened, the sample thawed, and the solvent together with other volatiles transferred into the cold traps at 100 mPa during 1.5 h, thus separating them from the monoglycerides. A high vacuum was avoided to minimize carry-over of monoglycerides into the cold traps. The distillate containing the aroma compounds was then dried over anhydrous Na_2SO_4 and concentrated to 2 mL on a Vigreux column (50 cm × 1 cm) and finally to 0.5 mL under a gentle stream of nitrogen.

Quantification of Volatiles. *(i) Furfural / Cysteine Reaction.* The diethyl ether used for the isolation of volatiles was spiked with benzylmercaptan as internal standard (5 or 10 μg).

(ii) Ribose / Cysteine Reaction. The diethyl ether was spiked with the following amounts of standard compounds: 350 μg

Motif Exhibit 1093, Page 10 of 17

Case No.: IPR2023-00209
U.S. Patent No. 10,039,306

of 5-methylfurfural for quantitation of MFT, FFT, and furfural; 350 μg of 5-ethyl-4-methyl-3-hydroxy-2(5*H*)-furanone (abhexon) for quantitation of 4-hydroxy-5-methyl-3(2*H*)-furanone (norfuraneol); and 4.7 μg of 3-acetyl-2,5-dimethylthiophene for quantitation of bis(2-methyl-3-furyl) disulfide (MFT−MFT).

Quantitation in both reactions was based on the ratio of peak areas using the FID trace and was not corrected for possible differences in FID responses and recovery yields of internal standard and analyte.

High-Resolution Gas Chromatography (HRGC) and HRGC Mass Spectrometry (HRGC-MS). An HP5890 GC equipped with a DB-1701 fused silica capillary column (J&W, Folsom, CA; 30 m × 0.32 mm × 0.25 μm) was used. By means of a Valco valve, the effluent (He used as carrier gas; 80 kPa) was split to an FID and an FPD detector, both kept at 250 °C. An aliquot (1 μL) of the concentrated samples was injected in the splitless mode using an HP-7673A autosampler. Identification of compounds was performed using an HP-5890 series 2 GC with a DB-5 capillary column (J&W; 30 m × 0.32 mm × 0.25 μm) connected to a Finnigan MAT SSQ 7000 mass spectrometer. Mass spectra in the electron impact mode were generated at 70 eV and in the chemical ionization mode at 150 eV with isobutane as reagent gas. The GC oven temperature was programmed from 20 °C (2 min) at 70 °C/min to 50 °C (2 min), at 6 °C/min to 180 °C, and finally at 20 °C/min to 240 °C (10 min). Linear retention indices (RI) were calculated according to the method of van den Dool and Kratz (1963).

RESULTS

Furfural and Cysteine as Precursors of FFT. In the first series of experiments, cysteine was heated with furfural. Maillard reactions are often studied at elevated temperatures of 140−180 °C. In our study 100 °C was chosen due to the necessity to stay in the cubic phase region of the Dimodan PV (80−120 °C) and to avoid the use of pressurizable reaction vessels.

The cubic phase of the Dimodan PV/water system (80:20), used in this study, reverses to an L_2 microemulsion at temperatures > 120 °C (Krog, 1998). It is also known that cubic to hexagonal and hexagonal to L_2 phase transition temperatures decrease for unsaturated monoglycerides, such as Dimodan LS. Thus, by keeping the monoglyceride/water at a constant ratio (80:20) and maintaining the temperature at 100 °C, we could obtain a reversed microemulsion phase by replacing Dimodan PV with Dimodan LS (Figure 1).

Reaction in Water. Figure 2 shows GC/FPD chromatograms of volatile compounds obtained from cysteine/furfural mixtures reacted in different media (water, microemulsion, and cubic phase).

In the aqueous phase (Figure 2A), besides the standard benzylmercaptane, only two sulfur compounds were detected in trace amounts. One compound was identified as FFT on the basis of its the retention index (RI) and MS spectra. It is the expected product from the reaction of furfural with cysteine.

Reaction in Structured Fluids. The yield of FFT was significantly increased in both the microemulsion and the cubic phase. In addition, two new compounds were detected in relatively large amounts (Figure 2B,C) with RI values of 1521 and 1997 on a DB-1701 gas capillary column.

On the basis of MS/EI (Figure 3) and MS/CI, these two molecules were identified as 2-(2-furyl)thiazolidine (RI = 1521) and, tentatively, *N*-(2-mercaptovinyl)-2-(2-furyl)thiazolidine (RI = 1997). To confirm these structures, 2-(2-furyl)thiazolidine was prepared from furfural and cysteamine in aqueous solution by heating an equimolar mixture (20 mmol each) at 100 °C for 1 h (Figure 4). The mass spectrum of the synthesized compound was in good agreement with the spectrum of the unknown compound at RI = 1521.

Both compounds, *N*-(2-mercaptovinyl)-2-(2-furyl)thiazolidine and 2-(2-furyl)thiazolidine, as well as FFT were quantified in the three systems investigated (Table 1). On the basis of the relative peak areas to the internal standard benzylmercaptane, ~2 μg of FFT was generated in the aqueous reaction system. Under the same conditions ~9 μg of FFT was generated in a microemulsion and ~12 μg in the cubic structure, resulting in a 6-fold increase compared to the aqueous system.

The same trend was observed for 2-(2-furyl)thiazolidine and *N*-(2-mercaptovinyl)-2-(2-furyl)thiazolidine, for which the cubic phase as matrix gave the highest amounts of 240 and 123 μg, respectively. In the aqueous solution, 2-(2-furyl)thiazolidine was detectable in only one sample, whereas *N*-(2-mercaptovinyl)-2-(2-furyl)-thiazolidine could not be detected under the experimental conditions. These results indicate that the cubic structure is the most efficient matrix for the generation of these three volatile compounds under the chosen reaction conditions. Moreover, the ratio of the amount for each compound formed in the cubic phase and in the microemulsion differed significantly. Compared to the microemulsion, the amount of *N*-(2-mercaptovinyl)-2-(2-furyl)thiazolidine was 10 times higher in the cubic phase, whereas ratios of about 1.3 and 6 were observed for FFT and 2-(2-furyl)thiazolidine, respectively. Possible reasons for the different reaction yields will be discussed later.

A hypothetical pathway for the generation of 2-(2-furyl)thiazolidine from furfural (**I**) and cysteine (**II**) is displayed in Figure 5. The first step in the reaction is the addition of cysteine to the carbonyl group of furfural. The subsequent elimination of a molecule water gives rise to a Schiff base (**III**). This compound may undergo decarboxylation, resulting in product (**IV**). This intermediate can finally form a five-membered ring by addition of the nucleophilic sulfur to the imine, which leads to the formation of 2-(2-furyl)thiazolidine. Compound **III** may also first cyclize to compound **IIIb** and subsequently lose CO_2. The 2-(2-furyl)thiazolidine may then react with mercaptoacetaldehyde, released from cysteine upon Strecker degradation, to finally give rise to the tentatively identified *N*-(2-mercaptovinyl)-2-(2-furyl)thiazolidine.

Ribose/Cysteine Reaction. This system was chosen because many parameters influencing flavor generation such as pH, water activity, and temperature have already been studied (Hofmann and Schieberle, 1995) and because of the importance of C5 sugars in the formation of meatlike and savory flavors. In the following, we selectively determined potent odorants that could be identified under the analytical conditions rather than giving an entire view of volatiles generated.

The sensory properties of the reaction flavor obtained in the aqueous system were compared with those of the cubic phase sample by using a laboratory panel. The reaction carried out in the cubic phase was found to have a more intense overall flavor with a strong rubber, eggy, roast chicken-like aroma. The aroma of the aqueous reaction was evaluated after transformation of the solution into a cubic phase system in order to have similar volatile−matrix interactions. This mixture was weak in aroma, reminiscent of meat and lard with some burnt character.

Case No.: IPR2023-00209
U.S. Patent No. 10,039,306

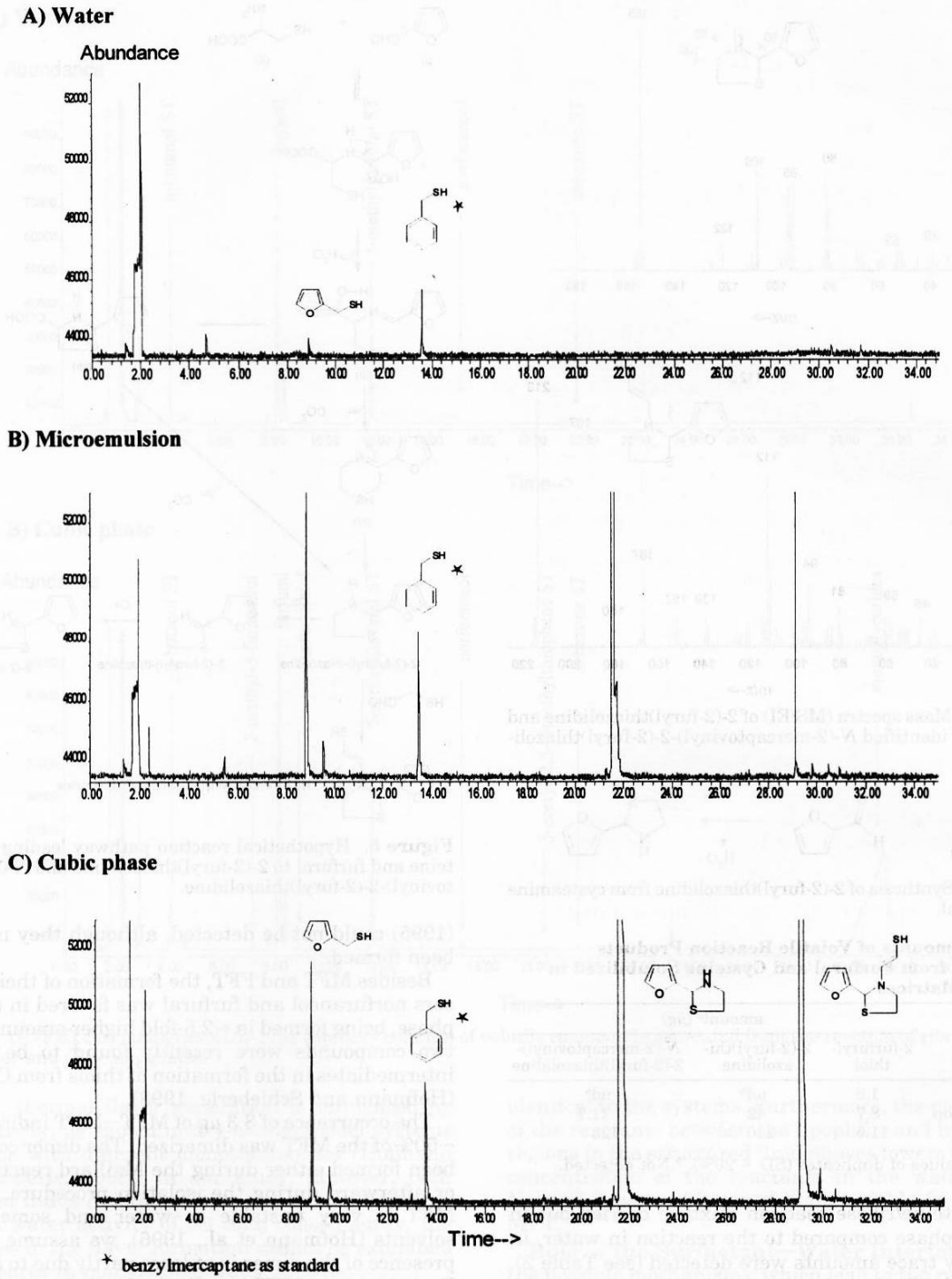

Figure 2. GC/FPD chromatogram (DB-1701 capillary column) of volatile compounds generated from the reaction of furfural/cysteine in (A) water, (B) microemulsion, and (C) cubic phase. The internal standard benzylmercaptane is indicated by ★.

The volatiles formed in the cubic phase and in water were monitored by GC/FID (Figure 6) and GC/FPD (Figure 7). The FPD chromatograms evidenced the differences between the two samples indicating generation of higher amounts of sulfur-containing compounds in the cubic system.

A multiple standard addition method was used to quantify six compounds in the reaction mixtures that were identified by comparison with the corresponding reference compounds based on RI on two capillary columns of different polarities (DB-5 and DB-1701) and their MS/EI spectra. Three compounds, covering the range of chemical and physical properties of the volatiles generated in the Maillard reaction, were chosen as internal standards (see Experimental Procedures). Possible differences in recovery yield of the analyte and the standard were not taken into account for the calculation of concentrations.

Similarly to the reaction of cysteine/furfural, there was a significant increase in the concentration of FFT

Motif Exhibit 1093, Page 12 of 17

Case No.: IPR2023-00209
U.S. Patent No. 10,039,306

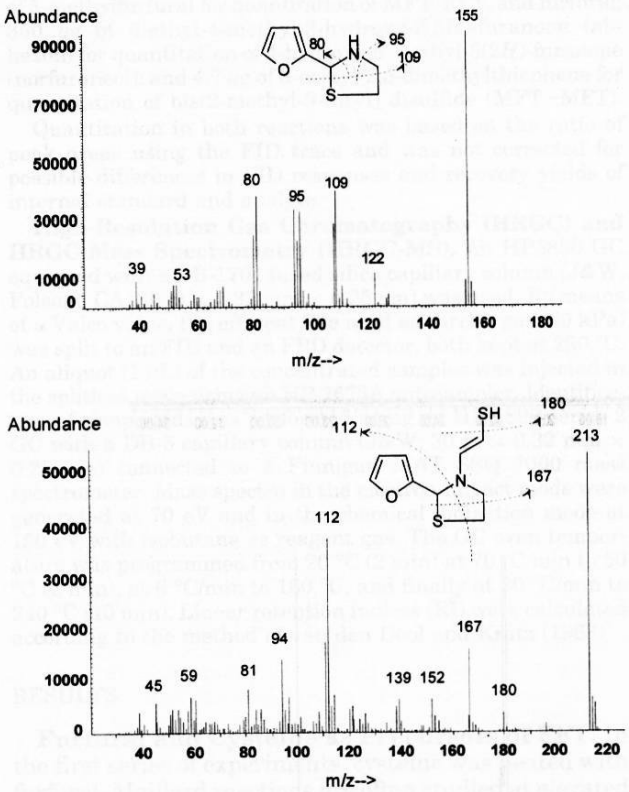

Figure 3. Mass spectra (MS/EI) of 2-(2-furyl)thiazolidine and tentatively identified *N*-(2-mercaptovinyl)-2-(2-furyl)thiazolidine.

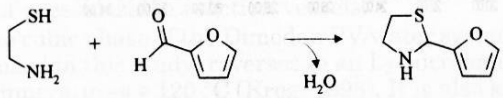

Figure 4. Synthesis of 2-(2-furyl)thiazolidine from cysteamine and furfural.

Table 1. Amounts of Volatile Reaction Products Generated from Furfural and Cysteine Solubilized in Different Matrices

matrix	amount[a] (μg) 2-furfuryl-thiol	2-(2-furyl)thi-azolidine	*N*-(2-mercaptovinyl)-2-(2-furyl)thiazolidine
water	1.8	nd[b]	nd[b]
microemulsion	8.7	42	11.7
cubic phase	11.6	240	123

[a] Mean values of duplicates (SD < 20%). [b] Not detected.

in the cysteine/ribose reaction mixture carried out in the cubic phase compared to the reaction in water, in which only trace amounts were detected (see Table 2). The detection limit under the given conditions was ~0.5 μg/5 g of cubic phase sample. The potent odorant MFT was detected only in the cubic phase system. The absence of this compound in the reference is surprising, but not contradictory to the findings in the literature (Hofmann and Schieberle, 1995). Indeed, this compound was detectable in the reference when the reaction system was directly extracted with diethyl ether, that is, no cubic phase was formed before extraction, and when the isolation of volatiles was done by vacuum distillation. The losses and poor recovery during isolation from the cubic phase also explain that some of the other odorants reported by Hofmann and Schieberle

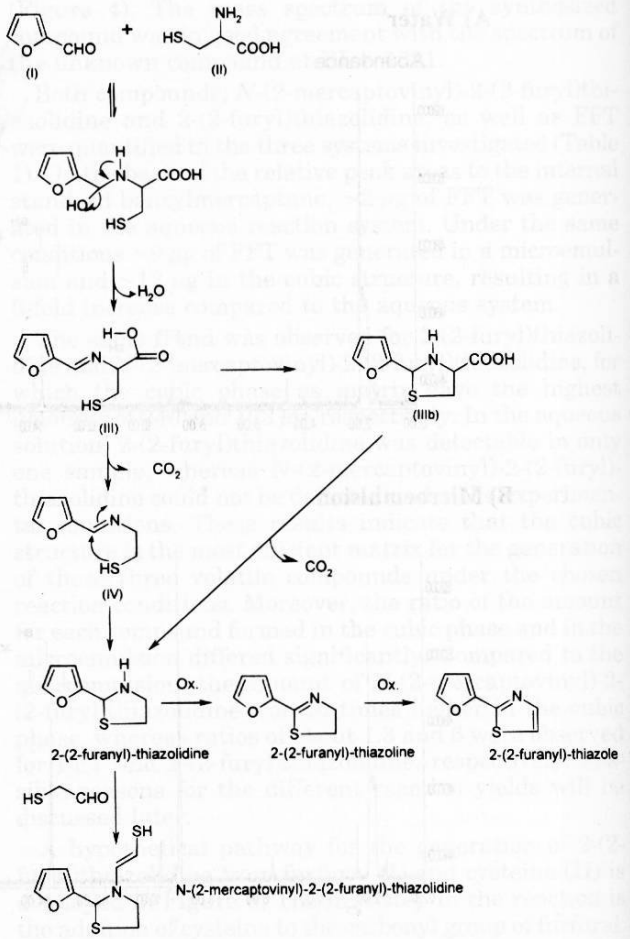

Figure 5. Hypothetical reaction pathway leading from cysteine and furfural to 2-(2-furyl)thiazolidine and *N*-(2-mercaptovinyl)-2-(2-furyl)thiazolidine.

(1995) could not be detected, although they may have been formed.

Besides MFT and FFT, the formation of their precursors norfuraneol and furfural was favored in the cubic phase, being formed in ~2.5-fold higher amounts. These two compounds were recently found to be the key intermediates in the formation of thiols from C5 sugars (Hofmann and Schieberle, 1998).

The occurrence of 8.3 μg of MFT−MFT indicates that ~50% of the MFT was dimerized. The dimer could have been formed either during the Maillard reaction itself or afterward during the isolation procedure. Because MFT is very unstable in water and some organic solvents (Hofmann et al., 1996), we assume that the presence of the dimer is at least partly due to artifacts. Partitioning of MFT into the hydrophobic chain region of the cubic phase could be the reason for its enhanced generation.

DISCUSSION

This work clearly demonstrates that structured fluids, such as association colloids, strongly influence the thermal generation of volatiles from cysteine/furfural and cysteine/ribose mixtures. Various hypotheses will be discussed in an attempt to gain a first understanding of these phenomena.

Water Activity. The Maillard reaction is known to be dependent on water activity (Bell and Labuza, 1994).

Motif Exhibit 1093, Page 13 of 17

Case No.: IPR2023-00209
U.S. Patent No. 10,039,306

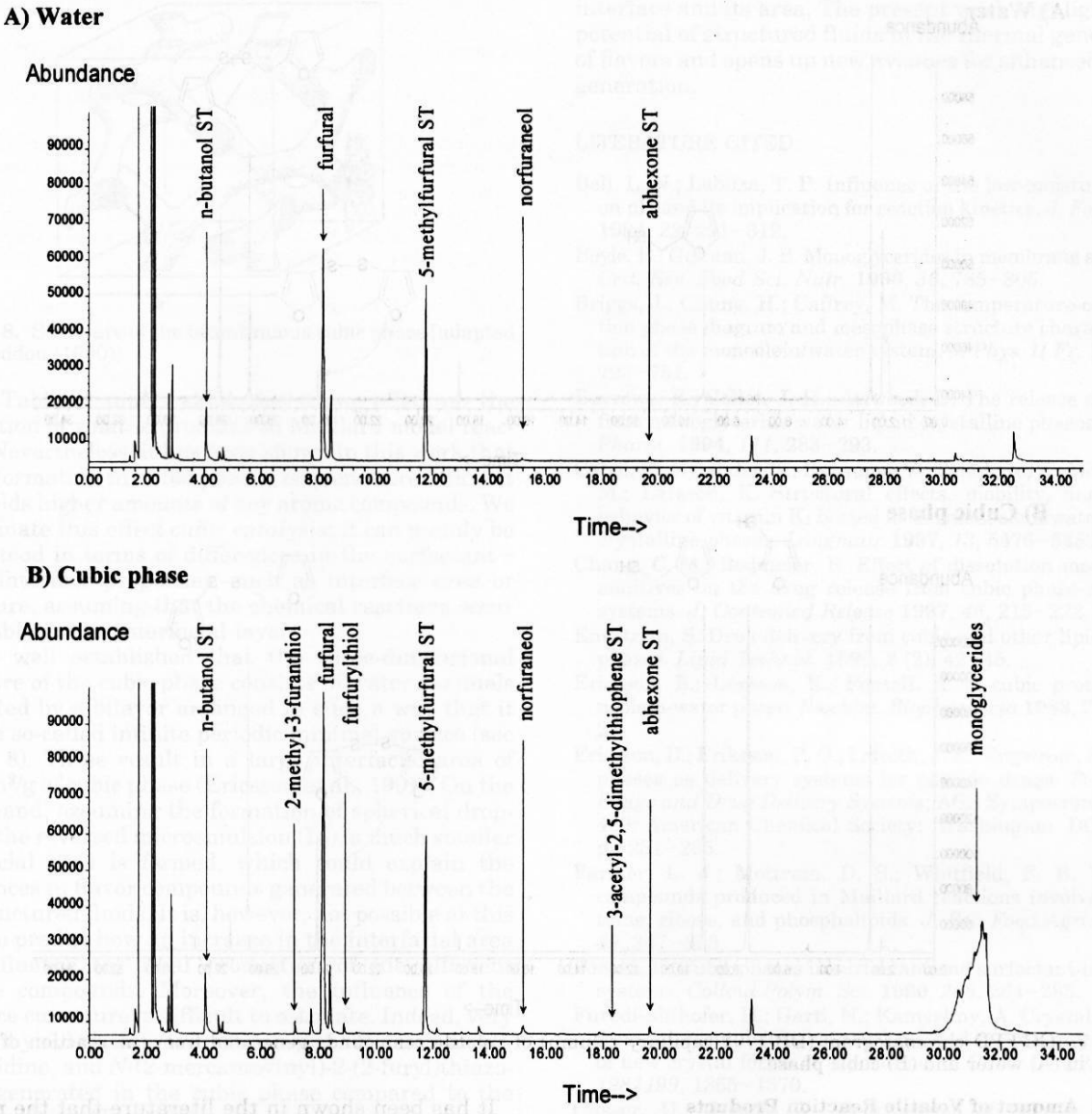

Figure 6. GC/FID chromatogram (DB-1701 capillary column) of volatile compounds generated from the reaction of ribose/cysteine in (A) water and (B) cubic phase.

Likewise, thermal flavor generation is influenced by water activity, as shown in dry-heated model systems of cysteine with different monosaccharides (Hofmann and Schieberle, 1998). In our study, however, both structured fluids (microemulsion and cubic phase) exhibited a water activity of ~1 and, consequently, the differences in the flavor formation cannot be explained by differences in macroscopic water activity.

Reaction pathways may, however, depend on water and reactant mobility and their availability to each other. In aqueous solutions, the reactants are totally free to interact, whereas in the investigated structured fluids the water is confined within cubic phase channels or the internal core of the microemulsion, respectively.

Often, it has been shown that rate enhancement is primarily due to an increase of reactant concentration in the water droplet (Holmberg, 1994; Tascioglu, 1996). In this study, furfural and cysteine were entirely solubilized in water before the different systems (cubic phase and microemulsion) were prepared, and their concentrations were based on the water content being identical in the systems. Furthermore, the partitioning of the reactants between the lipophilic and hydrophilic regions in the structured fluid phases lowers the actual concentration of the reactants in the water region. Nevertheless, we observed higher yields for FFT and MFT.

Role of the Surfactant—Water Interface. One of the possible mechanisms, which lead to the remarkable rate enhancement and to different product distribution, is the partitioning (compartmentalization) of the reactants at the surfactant−water interface or close to it, thus inducing a concentration gradient. Locally high concentrations at the interface are thought to strongly accelerate bimolecular reactions. Moreover, the close proximity of the reactants as well as their restrained movement within the interface will increase the frequency of molecular collisions (cage effect).

This hypothesis is quite coherent with previous results demonstrating that aspartame, a dimeric amino acid, is clearly solubilized at the interface of microemulsions (Furedi-Milhofer et al., 1999). Moreover, it was

Motif Exhibit 1093, Page 14 of 17

Case No.: IPR2023-00209
U.S. Patent No. 10,039,306

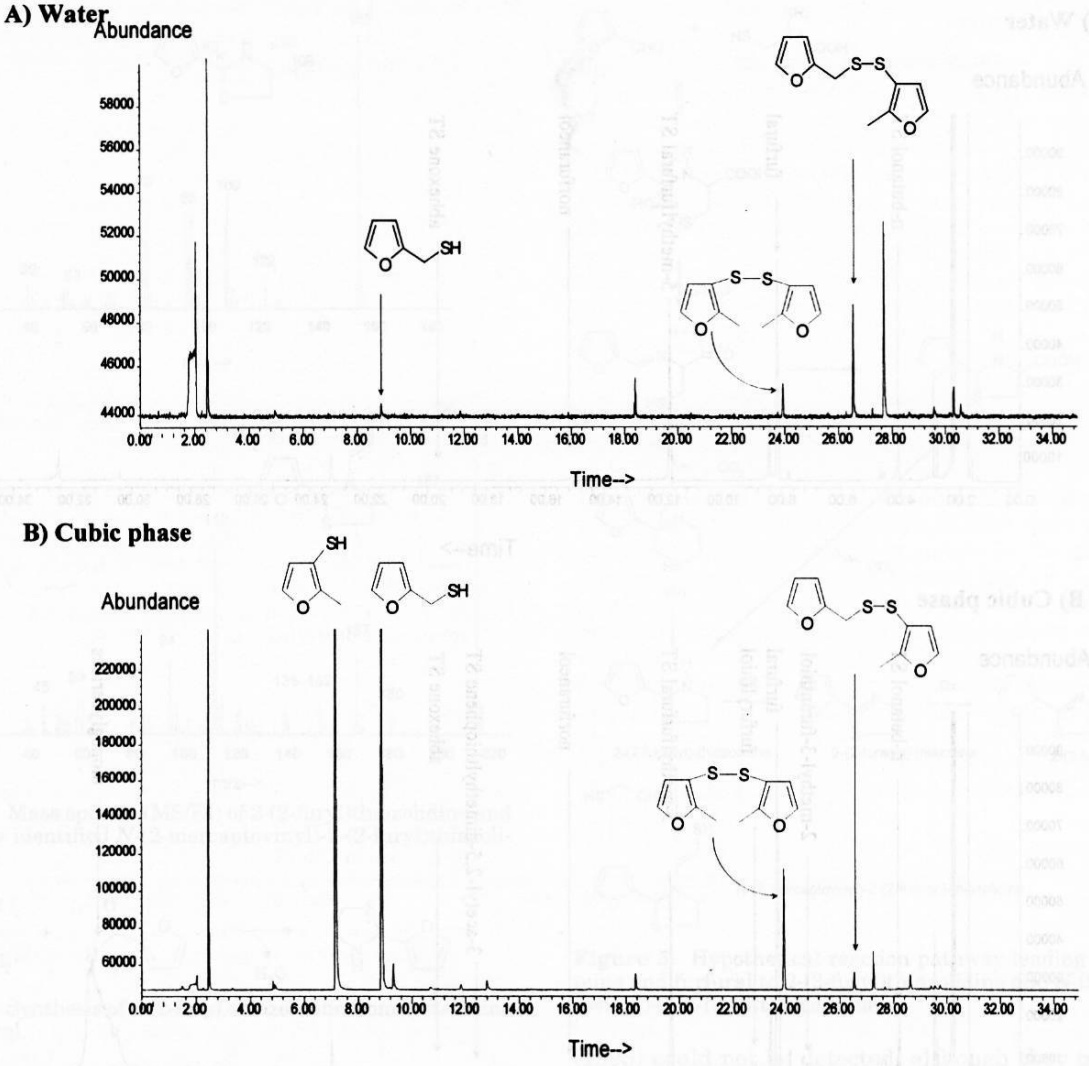

Figure 7. GC/FPD chromatogram (DB-1701 capillary column) of volatile compounds generated from the reaction of ribose/cysteine in (A) water and (B) cubic phase.

Table 2. Amount of Volatile Reaction Products Generated from Ribose and Cysteine Solubilized in Different Matrices

compound[b]	amount[a] (μg) cubic phase	water
2-methyl-3-furanthiol (MFT)	18.4	nd[c]
2-methyl-3(2*H*)-furanone	36.7	13.1
furfural	874	351
2-furfurylthiol (FFT)	12.0	tr[d]
3-mercapto-2-pentanone	tr	nd[c]
norfuraneol	698	291
MFT−MFT	8.3	tr
MFT−FFT	tr	tr

[a] Mean values of duplicates (SD < 20%). [b] Compounds were identified by comparison with the reference compound based on retention indices on DB-5, DB-1701, and MS/EI spectra. [c] Not detected.

shown that even water-soluble molecules such as butanedione can induce a phase transition of the cubic phase into a lamellar phase due to interactions with the monoglyceride surfactant headgroup (Vauthey, 1998). Therfore, one may expect that cysteine, like aspartame or butanedione, will equally penetrate into the interface and will be localized or immobilized at the interface.

It has been shown in the literature that the release of H_2S from cysteine solution at pH 3−9 shows a first-order reaction enhanced by alkaline pH (Zheng and Ho, 1994). The activation energies are 31.3 and 29.4 kcal/mol for pH 3.0 and 9.0, respectively. On the other hand, H_2S release activation energies from glutathione were 18.8 and 19.9 kcal/mol at pH 3 and 9, respectively. Glutathione evolves H_2S more rapidly than cysteine. In this case, the negative charge of the carboxyl group is further away from the α-carbon than it is in cysteine (Zheng and Ho, 1994). Therefore, the hydrogen atom of the α-carbon is more readily abstracted. If cysteine is attracted to the surface, its negative charge will be embedded in the bilayer and will appear to be more distant to the α-carbon than it is in free cysteine. As a result, the pathway leading to the formation of FFT will become more favorable, as observed in our experiments.

Therefore, besides a concentration effect, the specific microenvironment at the surfactant−water interface may influence the transition state by lowering the activation energy (Tascioglu, 1996) and lead to a rate enhancement in the generation of volatiles.

Role of the Interfacial Area. Rate enhancement occurring in microemulsions is generally referred to as *microemulsion catalysis* (Rathman, 1996; Romsted et al.,

Case No.: IPR2023-00209
U.S. Patent No. 10,039,306

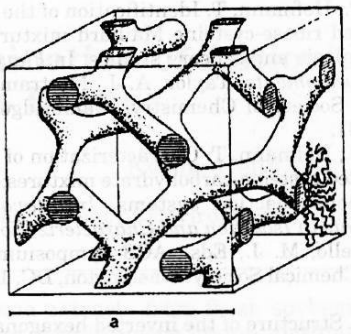

Figure 8. Structure of the bicontinuous cubic phase [adapted from Seddon (1990)].

1997). Tables 1 and 2 show the strong effect on the generation of volatile products in Maillard model reactions. Nevertheless, it has been shown in this work that flavor formation in cubic phases is even more efficient and yields higher amounts of key aroma compounds. We denominate this effect *cubic catalysis*; it can mainly be understood in terms of differences in the surfactant–water interface properties, such as interface area or curvature, assuming that the chemical reactions occur preferably at the interfacial layer.

It is well established that the three-dimensional structure of the cubic phase consists of water channels separated by a bilayer arranged in such a way that it forms a so-called infinite periodic minimal surface (see Figure 8). These result in a large interfacial area of ~400 m^2/g of cubic phase (Ericsson et al., 1991). On the other hand, assuming the formation of spherical droplets in the reversed microemulsion (L_2), a much smaller interfacial area is formed, which could explain the differences in flavor compounds generated between the two structured fluids. It is, however, not possible at this stage to predict how an increase in the interfacial area will influence the final production of the different volatile compounds. Moreover, the influence of the interface curvature is difficult to estimate. Indeed, very different yield ratios were obtained for FFT, 2-(2-furyl)-thiazolidine, and *N*-(2-mercaptovinyl)-2-(2-furyl)thiazolidine generated in the cubic phase compared to the microemulsion (Table 1).

Additional information on the binding constants of the reactants and the products is required to gain a more precise insight into the distribution of compounds between the aqueous phase and the interface.

CONCLUSIONS

Monoglycerides/water systems forming bicontinuous cubic phases as well as microemulsions have been used as "microreactors" for the generation of aroma compounds by the Maillard reaction.

It was shown that structured fluids which are organized on a nanometer scale can lead to remarkably higher yields of FFT and MFT as well as different aroma profiles in the thermal generation of volatile compounds. The flavor enhancement is partly due to an increase in the reaction yield of odor-active compounds and partly due to the wider variety of reaction products formed in these structured media. Cubic phases showed a significantly higher flavor enhancement than microemulsions. However, both structured fluids were significantly more efficient as a reaction medium than water.

It is postulated that the dominant factors affecting the reaction yield are the nature of the water/surfactant interface and its area. The present work highlights the potential of structured fluids in the thermal generation of flavors and opens up new avenues for enhanced flavor generation.

LITERATURE CITED

Bell, L. N.; Labuza, T. P. Influenec of the low-moisture state on pH and its implication for reaction kinetics. *J. Food Eng.* **1994**, *22*, 291–312.

Boyle, E.; German, J. B. Monoglycerides in membrane systems. *Crit. Rev. Food Sci. Nutr.* **1996**, *36*, 785–805.

Briggs, J.; Chung, H.; Caffrey, M. The temperature-composition phase diagram and mesophase structure characterization of the monoolein/water system. *J. Phys. II Fr.* **1996**, *6*, 723–751.

Burrows, R.; Collet, J. H.; Attwood, D. The release of drugs from monoglyceride-water liquid crystalline phases. *Int. J. Pharm.* **1994**, *111*, 283–293.

Caboi, F.; Nylander, T.; Razumas, V.; Talaikyte, Z.; Monduzzi, M.; Larsson, K. Structural effects, mobility, and redox behavior of vitamin K_1 hosted in the monoolein/water liquid crystalline phases. *Langmuir* **1997**, *13*, 5476–5483.

Chang, C.-M.; Bodmeier, R. Effect of dissolution media and additives on the drug release from cubic phase delivery systems. *J. Controlled Release* **1997**, *46*, 215–222.

Engstrom, S. Drug delivery from cubic and other lipid-water phases. *Lipid Technol.* **1990**, *2* (2), 42–45.

Ericsson, B.; Larsson, K.; Fontell, K. A cubic protein-monoolein-water phase. *Biochim. Biophys. Acta* **1983**, *729*, 23–27.

Ericsson, B.; Eriksson, P. O.; Lofroth, J. E.; Engstrom, S. Cubic phases as delivery systems for peptide drugs. *Polymeric Drugs and Drug Delivery Systems*; ACS Symposium Series 469; American Chemical Society: Washington, DC, 1991; pp 251–265.

Farmer, L. J.; Mottram, D. S.; Whitfield, F. B. Volatile compounds produced in Maillard reactions involving cysteine, ribose, and phospholipids. *J. Sci. Food Agric.* **1989**, *49*, 347–368.

Fontell, K. Cubic phases in surfactant and surfactant-like lipid systems. *Colloid Polym. Sci.* **1990**, *268*, 264–285.

Furedi-Milhofer, H.; Garti, N.; Kamyshny, A. Crystallization from microemulsions—a novel method for the preparation of new crystal forms of aspartame. *J. Cryst. Growth* **1999**, *198/199*, 1365–1370.

Gasser, U.; Grosch, W. Identification of volatile flavour compounds with high aroma values from cooked beef. *Z. Lebensm. Unters. Forsch.* **1988**, *186*, 489–494.

Hiemenz, P. C. *Principles of Colloid and Surface Chemistry*; Dekker: New York, 1986.

Hofmann, T.; Schieberle, P. Evaluation of the key odorants in a thermally treated solution of ribose and cysteine by aroma extract dilution techniques. *J. Agric. Food Chem.* **1995**, *43*, 2187–2194.

Hofmann, T.; Schieberle, P. Studies on intermediates generating the flavor compounds 2-methyl-3-furanthiol, 2-acety-2-thiazoline and sotolone by Maillard-type reactions. In *Flavour Science—Recent Developments*; Taylor, A. J., Mottram, D. S., Eds.; The Royal Society of Chemistry: Cambridge, U.K., 1996; pp 182–187.

Hofmann, T.; Schieberle, P. Quantitative model studies on the effectiveness of different precursor systems in the formation of the intense odorants 2-furfurylthiol and 2-methyl-3-furanthiol. *J. Agric. Food Chem.* **1998**, *46*, 235–241.

Hofmann, T.; Schieberle, P.; Grosch, W. Model studies on the oxidative stability of odour-active thiols occurring in food flavors. *J. Agric. Food Chem.* **1996**, *44*, 251–255.

Holmberg, K. Organic and bioorganic reactions in microemulsions. *Adv. Colloid Interface Sci.* **1994**, *51*, 137–174.

Holscher, W.; Vitzthum, O. G.; Steinhart, H. Identification and sensorial evaluation of aroma-impact-compounds in roasted Colombian coffee. *Cafe Cacao The* **1990**, *34*, 205–212.

Motif Exhibit 1093, Page 16 of 17

Case No.: IPR2023-00209
U.S. Patent No. 10,039,306

Krog, N. Food emulsifiers and their chemical and physical properties. In *Food Emulsions*; Friberg, S., Larsson, K., Eds.; Dekker: New York, 1997.

Larsson, K. Cubic lipid-water phases: Structures and biomembrane aspects. *J. Phys. Chem.* **1989**, *93*, 7304–7314.

Larsson, K. *Lipids—Molecular Organization, Physical Functions and Technical Applications*; The Oily Press: Dundee, U.K., 1994.

Laughlin, R. G. *The Aqueous Phase Behavior of Surfactants*; Academic Press: San Diego, CA, 1994.

Mottram, D. S.; Whitfield, F. B. Volatile compounds from the reaction of cysteine, ribose, and phospholipids in low-moisture systems. *J. Agric. Food Chem.* **1995**, *43*, 984–988.

Mulders, E. J. Volatile components from the non-enzymatic browning reaction of the cysteine/cystine-ribose system. *Z. Lebensm. Unters. Forsch.* **1973**, *152*, 193–201.

Münch, P.; Hofmann, T.; Schieberle, P. Comparison of key odorants generated by thermal treatment of commercial and self-prepared yeast extracts: influence of the amino acid composition on odorant formation. *J. Agric. Food Chem.* **1997**, *45*, 1338–1344.

Osborne, D. W.; Ward J. I. Lyotropic liquid crystals as topical drug delivery vehicles. *Int. J. Pharm. Adv.* **1995**, *1* (1), 38–45.

Rathman, J. F. Micellar catalysis. *Curr. Opin. Colloid Interface Sci.* **1996**, *1*, 514–518.

Razumas, V.; Larsson, K.; Miezis, Y.; Nylander T. A cubic monoolein-cytochrome *c*-water phase: X-ray diffraction, FT-IR, differential scanning calorimetric, and electrochemical studies. *J. Phys. Chem.* **1996**, *100*, 11766–11774.

Romsted, L. S.; Bunton, C. A.; Yao, J. Micellar catalysis, a useful misnomer. *Curr. Opin. Colloid Interface Sci.* **1997**, *2*, 622–628.

Schieberle, P. Studies on the flavour formation of roasted white sesame seeds. In *Progress in Flavour and Precursor Studies*; Schreier, P., Winterhalter, P., Eds.; Allured Publishers: Wheaton, IL, 1993; pp 343–360.

Schieberle, P.; Hofmann, T. Identification of the key odorants in processed ribose-cysteine Maillard mixtures by instrumental analysis and sensory studies. In *Flavour Science—Recent Developments*; Taylor, A. J., Mottram, D. S., Eds.; The Royal Society of Chemistry: Cambridge, U.K., 1996; pp 175–181.

Schieberle, P.; Hofmann, T. Characterization of key odorants in dry-heated cysteine-carbohydrate mixtures: Comparison with aqueous reaction systems. In *Flavor Analysis—Developments in Isolation and Characterization*; Mussinan, C. J., Morello, M. J., Eds.; ACS Symposium Series 705; American Chemical Society: Washington, DC, 1998; pp 320–330.

Seddon, J. M. Structure of the inverted hexagonal phase, and non-lamellar phase transitions of lipids. *Biochim. Biophys. Acta* **1990**, *1031*, 1–69.

Sen, A.; Laskawy, G.; Schieberle, P.; Grosch, W. Quantitative determination of β-damascenone in foods using a stable isotope dilution assay. *J. Agric. Food Chem.* **1991**, *39*, 757–759.

Tascioglu, S. Micellar solutions as reaction media. *Tetrahedron* **1996**, *52*, 11113–11152.

Van den Dool, H.; Kratz, P. A generalization of the retention index system including linear temperature programmed gas–liquid partition chromatography. *J. Chromatogr.* **1963**, *24*, 463–471.

Vauthey, S. Solubilization of flavour compounds in structured fluids. Ph.D. Thesis, University of Lausanne, 1998.

Zheng, Y.; Ho, C.-T. Kinetics of the release of hydrogen sulfide from cysteine and glutathione during thermal treatement. In *Sulfur Compounds in Foods*; Mussinan, C. J., Keelan, M. E., Eds.; ACS Symposium Series 564; American Chemical Society: Washington, DC, 1994.

Received for review November 19, 1999. Revised manuscript received June 5, 2000. Accepted June 5, 2000.

JF991254A

Motif Exhibit 1093, Page 17 of 17